On-Wafer Calibration Algorithm for Partially Leaky Multiport Vector Network Analyzers

Valeria Teppati, *Member, IEEE,* and Andrea Ferrero, *Member, IEEE*

***Abstract*—A new solution for multiport vector network analyzer calibration is presented in this paper. The error model is divided in two separate leaky halves, each of them with crosstalk terms, but without the leakage between the two sides. This error model is particularly useful for on-wafer measurements, when multisignal probes are employed and the crosstalk among probe fingers may dramatically affect the measurement accuracy. We will show that, with a simple choice of calibration standards, the new procedure takes the same time of a classical two-port line-reflect-match or thru-reflect-line calibration. The proposed algorithm is verified with measurements and simulations in both coaxial and on-wafer environments.**

***Index Terms*—Leaky calibration, leaky error model, multiport calibration, multiport error model, multiport S-parameters, multiport vector network analyzer (VNA), on-wafer calibration.**

I. Introduction

OVER THE last years, multiport measurements have spread from microwave and RF devices to signal integrity of digital integrated circuits (ICs). The great complexity of circuits and systems in almost every microwave application has generated new challenges and tasks from the testing point-of-view [1], [2]. Historically, the problem of multiport measurements has been solved following two main philosophies: by taking an n-port scattering matrix from m-port measurements where $m < n$, connecting the remaining ports to known [3]–[6] or unknown [7] one-port loads or by using multiport vector network analyzers (VNAs) (typically four ports) with different architectures and options [8]–[15].

Although the calibration of multiport VNAs is a well-known and explored field [16]–[19], the development of complex ICs and the introduction of multifinger on-wafer probes brings new interest onto calibration techniques that can handle the crosstalk among probe fingers.

The traditional error models are divided into two main categories, which are: 1) **leaky**, where the crosstalk among **ALL** the ports is taken into account and 2) **nonleaky**, where the crosstalk among the ports is neglected.

The latter is the most common one since the number of error coefficients is only $4n-1$, and many calibration procedures for this case were developed, while few calibration procedures have been proposed for the leaky model, both in two-port [20]–[22] and multiport environments [17]–[19], [23], [24].

Manuscript received April 8, 2005.

The authors are with the Electronic Engineering Department, Politecnico di Torino, 10129 Turin, Italy (e-mail: valeria.teppati@polito.it).

Digital Object Identifier 10.1109/TMTT.2005.857100

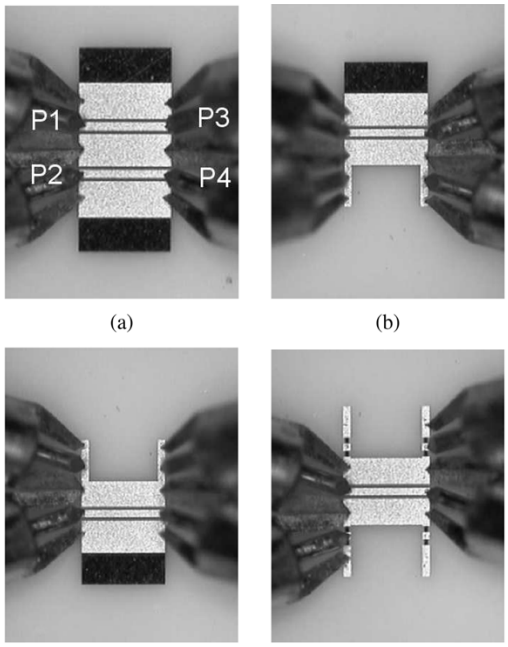

Fig. 1. Multifinger GSGGSG coplanar probes placed: (a) on a double coplanar waveguide and (b)–(d) on the on-wafer standards used during calibration.

However, both these traditional models fail in the particular situation of on-wafer multifinger probes, as sketched in Fig. 1. The **leaky** model requires a fixed and systematic crosstalk between the two halves, which cannot be accomplished unless the probes are kept fixed and the signal transmission through the air is assumed constant during the calibration and testing phase. The **nonleaky** model fails completely because it neglects crosstalk terms entirely. For those reasons, probe manufacturers designed multiground probes such as the ground–signal–ground–ground–signal–ground (GSGGSG) probes shown in Fig. 1 to reduce the crosstalk terms among fingers and make the nonleaky model applicable. Unfortunately, this solution constrains the test structure to a coplanar interface with the measurement system and prevents the use of simpler ground–signal–signal–ground probes where the crosstalk cannot be neglected at microwave frequencies.

In [25], a new multiport error model and its calibration procedure, called "half-leaky calibration," were introduced. In this model, the error coefficients are split into two separate leaky halves with the same number of ports. In [25], some preliminary verifications of the model and calibration procedure, performed in a coaxial environment, were shown. In this paper, we will present further and more complete on-wafer verifications, which highlight some new characteristics of the novel technique.

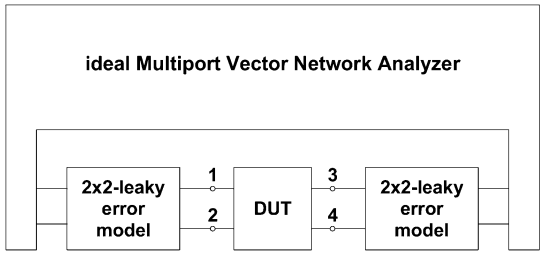

Fig. 2. Four-port half-leaky error model [25].

Once the half-leaky model is applied to four-port on-wafer measurements, the leakage among the fingers on the same probe is taken into account, while the side-by-side crosstalk is neglected, as sketched in Fig. 2. We will prove that, in this situation, this new model improves the accuracy against both the nonleaky model, as well as a fully leaky one. The crosstalk terms of the proposed half-leaky case are fixed and constant due to the fixed position of each probe finger, while the side-by-side crosstalk, which is usually minimal and difficult to model, is neglected. This is normally a better solution than trying a correction with the wrong terms as the full-leaky calibration, as proven in the following. Section II presents the mathematical formulation of the problem and an optimized calibration procedure where the number of required standard insertions is minimized. Section III shows the results of some measurements performed in a coaxial environment [25], aimed at the methodology validation, while Section IV shows the results of this new technique applied to on-wafer measurements.

II. Calibration Problem: Formulation and Solution

The problem is solved by simplifying the more general formulation for multiport leaky VNAs of [19]. Here, we revise the most important results of this theory to facilitate comprehension. Let us start from [19, eq. (3)]

$$\mathbf{KS_m - SLS_m + SH - M = 0} \tag{1}$$

where $\mathbf{S}$ and $\mathbf{S_m}$ are, respectively, the standard definitions and measurements and $\mathbf{K, L, M, H}$ are $n \times n$ full matrices of unknown calibration coefficients. This equation can be used for the deembedding, in the form

$$\mathbf{S} = (\mathbf{M - KS_m})(\mathbf{H - LS_m})^{-1} \tag{2}$$

or it can be used to compute the unknowns, once rewritten as a set of n^2 equations

$$-M_{ij} - \sum_{p=1}^{n} S_{ip}\left(\sum_{q=1}^{n} L_{pq}S_{mqj}\right) + \sum_{p=1}^{n} S_{ip}H_{pj} + \sum_{p=1}^{n} K_{ip}S_{mpj} = 0 \tag{3}$$

where $i = 1, \ldots, n, j = 1, \ldots, n$. Each standard connection (single port or multiport) provides a set of equations like (3), which can be collected into an homogeneous linear system, in the form

$$\mathbf{Cv} = 0 \tag{4}$$

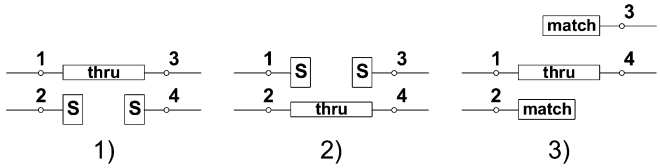

Fig. 3. Methodology for half-leaky two-port calibration in three steps (from [25]).

where $\mathbf{v} = [\mathrm{Col}\ (\mathbf{K})\mathrm{Col}\ (\mathbf{H})\mathrm{Col}\ (\mathbf{L})\mathrm{Col}\ (\mathbf{M})]^T$ is the unknown vector, the Col operator reorganizes a matrix into a vector [21], and $\mathbf{C}$ is a matrix containing only standard measurements and their definitions. To avoid the zero trivial solution, the system is normalized to one of the unknown coefficients, leading to an equation in the form $\mathbf{Nu} = \mathbf{g}$. In order to find a solution, the system requires a suitable number of independent equations, i.e., the rank of matrix $\mathbf{N}$ must be equal to or greater than the unknowns' number. This is achieved by carefully choosing the standards' set and their port connection; in [18], some criteria for such a combination for a nonleaky model were found. However, for this new half-leaky model, these rules cannot be applied, thus, a computer simulation of the test-set calibration was performed to determine the proper standard sequence.

We employed this formulation to solve the problem of a four-port $(n = 4)$ VNA modeled by two separate two-port leaky halves, as shown in Fig. 2. The total number of unknown calibration coefficients for a complete leaky problem would be $4n^2 - 1 = 63$, while for the half-leaky approach, it is reduced to $2n^2 - 1 = 31$ since half of the unknowns are assumed to be zero. If the ports are numbered so that 1 and 2 and 3 and 4 are the two leaky halves, according to the scheme in Fig. 2, then matrices $\mathbf{M, H, K, L}$ become block diagonal, as shown in the following:

$$\mathbf{M} = \begin{pmatrix} \tilde{\mathbf{M}}_{\mathbf{L}} & \mathbf{0} \\ \mathbf{0} & \tilde{\mathbf{M}}_{\mathbf{R}} \end{pmatrix} \tag{5}$$

where $\tilde{\mathbf{M}}_{\mathbf{L}}$ and $\tilde{\mathbf{M}}_{\mathbf{R}}$ are the left and right matrices. Matrix $\mathbf{C}$ is built applying (3) with half of the columns: the ones corresponding to the nonzero unknowns. For better insight on how the system is built up, an example for a four-port full-leaky and half-leaky model is given in the Appendix.

An optimized standard sequence, especially useful for on-wafer measurements, has been found and validated with simulations and measurements. Among the possible sequences, the one that has been adopted is similar to a classical line reflect mode (LRM) calibration, where connections of thrus, shorts, and 50-Ω loads are arranged such that **only three on-wafer probe placements** are required, as sketched in Fig. 3. The three standard combinations are: 1) thru ports 1–3 and shorts ports 2 and 4; 2) thru ports 2–4 and shorts ports 1 and 3; and 3) thru ports 1–4 and loads ports 2 and 3.

III. Coaxial Implementation and Tests of a Half-Leaky Multiport

Some experiments to validate the proposed methodology were performed on a four-port coaxial system [25]. The setup

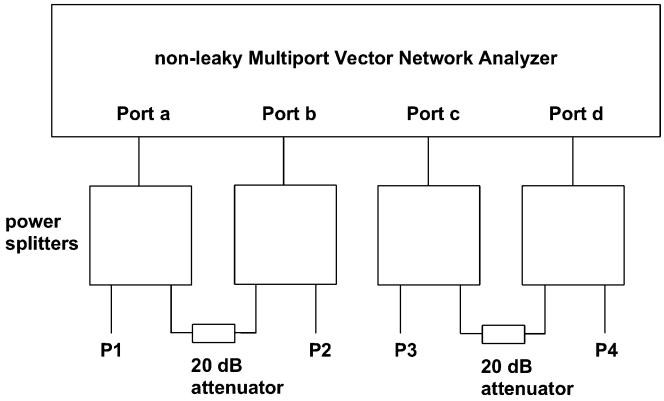

Fig. 4. Scheme of the multiport half-leaky system used in the experiments of Section III and in [25].

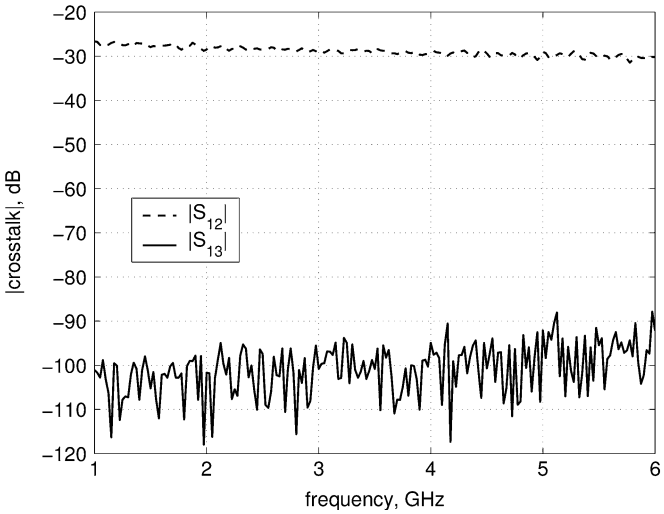

Fig. 5. Raw data [25] measured with unconnected ports. Introduced leakage mainly affects S_{12}, while S_{13} is unchanged.

sketched in Fig. 4 is based on a 6-GHz Anritsu W4623 coupled with a PAF MMS four-port expansion box. Furthermore, to simulate the crosstalk, two 20-dB attenuators, placed between ports a and b and ports c and d were introduced.

The analysis of raw data when all the ports are left open gives important information on the leakage amount. As shown in Fig. 5, the introduced leakage is conspicuous and mainly affects S_{12} (it changes from a negligible -100 to -20 dB), while S_{13} is unchanged.

First this multiport system has been calibrated, applying the standard sequence described above, and different devices have been measured. Offset shorts, matched loads, and attenuator measurements were performed in order provide a preliminary validation of the calibration procedure, and show very good results [25].

In Figs. 6 and 7, calibrated and raw data of a thru measured at ports 2 and 3 are reported; note that this thru connection was not employed during calibration, and this proves that the leakage error is completely removed.

Another comparison is shown in Fig. 8: here, the device, a 12-dB attenuator, was first connected to ports 1 and 2, then to

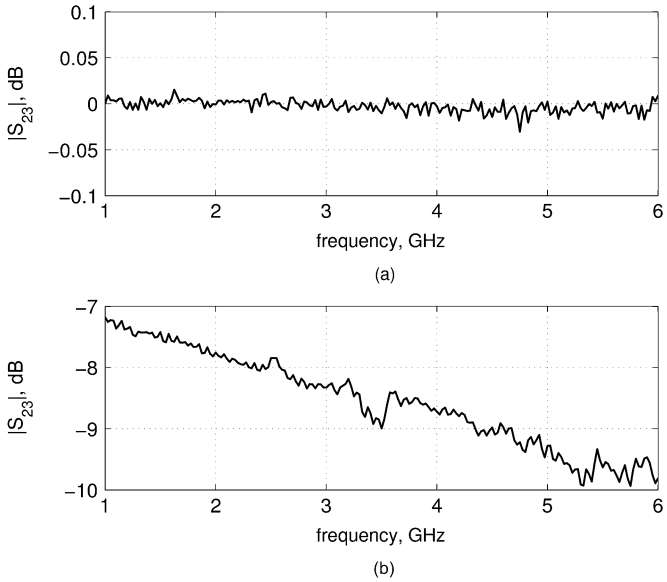

Fig. 6. Magnitude of thru connection between ports 2 and 3 (not used during calibration). (a) Corrected and (b) raw data. Data is from [25].

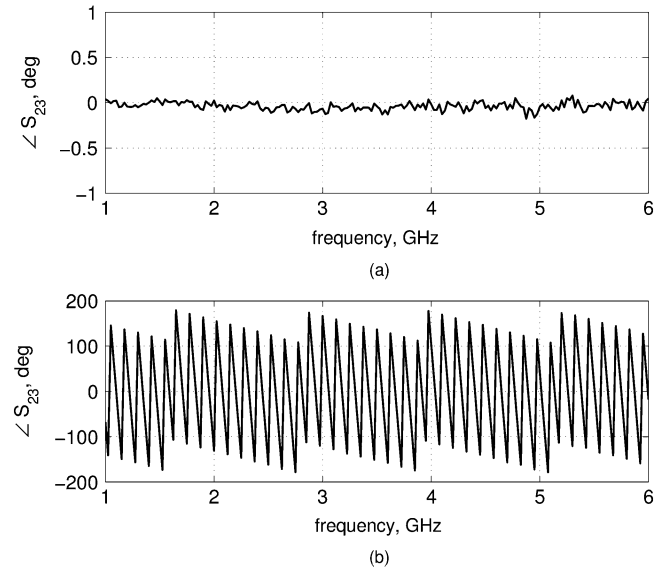

Fig. 7. Phase of thru connection between ports 2 and 3 (not used during calibration). (a) Corrected and (b) raw data phase. Data is from [25].

ports 2 and 4. In the first case, the leaky error coefficients are involved and the correction leads to the same results as the second one, although the initial raw data are clearly different.

IV. On-Wafer Implementation of a Half-Leaky Multiport

Here, we will show some results of the proposed calibration methodology with an actual on-wafer multiport system up to 18 GHz.

The test-set consists of an HP8510C combined with a PAF MMS expansion box to obtain a four-port multiport VNA, a Cascade Microtech Probe Station, and two GGB GSGGSG coaxial probes [see Fig. 1(a)]. Now, the leakage is due mainly to the crosstalk between the adjacent probe fingers, i.e., between ports 1 and 2 and ports 3 and 4.

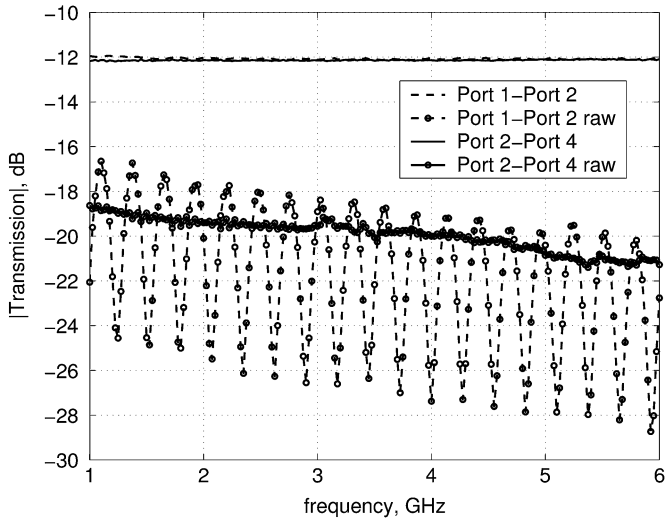

Fig. 8. 12-dB attenuator connected between ports 1 and 2 (nonleaky ports) and 2–4 (leaky ports). Corrected and raw data. Data is from [25].

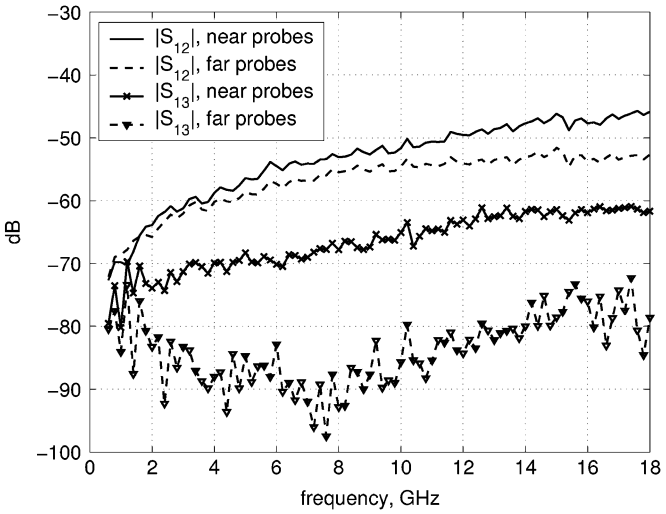

Fig. 9. Four open-circuit pads of Fig. 10(a) connected at ports 1–4 (raw data). The measurements were performed for two different distances between the probes (0.53 and 2 mm).

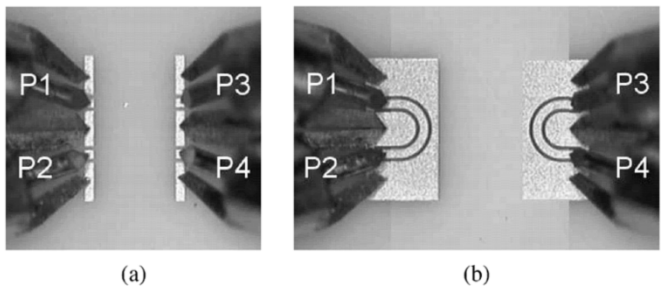

Fig. 10. (a) Open circuit-pads. (b) U-shaped lines.

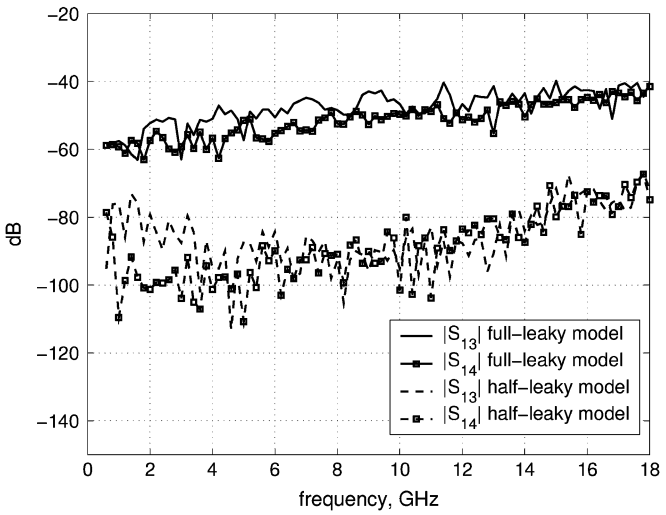

Fig. 11. Crosstalk parameters (S_{13} and S_{14}, probe distance is 2 mm) of the U-shaped line of Fig. 10(b). Comparison between full-leaky and half-leaky models.

The required calibration standards and some verification devices were realized on a special purpose substrate; the standard combination for the partially leaky calibration is the same as in Section III, i.e.: 1) thru ports 1–3 and shorts ports 2 and 4 of Fig. 1(b); 2) thru ports 2–4 and shorts ports 1 and 3 of Fig. 1(c); and 3) thru ports 1–4 and loads ports 2 and 3 of Fig. 1(d) where the first two connections are realized on the same physical standard by rotating the substrate by 180°.

One-port and multiport on-wafer verification devices were successfully used to provide preliminary validation of the calibration procedure. In the following, we will show the most significant results and, in particular, we will focus on the comparison of the half-leaky model with the nonleaky and full-leaky ones. The device-under-test (DUT)'s raw data are corrected with these three different sets of error coefficients, where the nonleaky ones are computed using the same set of standards implied for the half-leaky calibration, while the full-leaky ones are carried out adding four loads and four opens at ports 1–4.

Fig. 9 shows the raw measurements of four open-circuit pads on the coplanar calibration substrate [see Fig. 10(a)] for different distances between the contacted open pads, thus it provides an estimation of the amount of leakage between ports. When the probe pads are relatively far apart (2 mm), the crosstalk between ports 1–3 is negligible (<-70 dB), although it is still present between ports 1 and 2 (up to -55 dB @ 18 GHz). When the probes are close to each other (0.53 mm), the nonadjacent probe finger crosstalk $|S_{13}|$ dramatically rises up, while $|S_{12}|$ is almost unchanged.

Clearly the leakage between fingers of the same probe is greater than the leakage between different probes, and this is why a partially leaky model is a good choice. The full-leaky model is potentially prone to larger errors than the half-leaky model, when probe distance changes from the calibration to the measurement, since the amount of leakage heavily changes (Fig. 9).

The differences between the three models are most evident when comparing crosstalk parameters or loose couplings. A measurement of the crosstalk between two U-shaped transmission lines between ports 1 and 2 and 3 and 4 [depicted in Fig. 10(b)] is shown in Fig. 11. The probe distance is 2 mm. S_{13} and S_{14} are considerably degraded for the full-leaky model, whereas the partially leaky model gives the correct result of <-70-dB crosstalk. This is the effect of a miscorrection of the

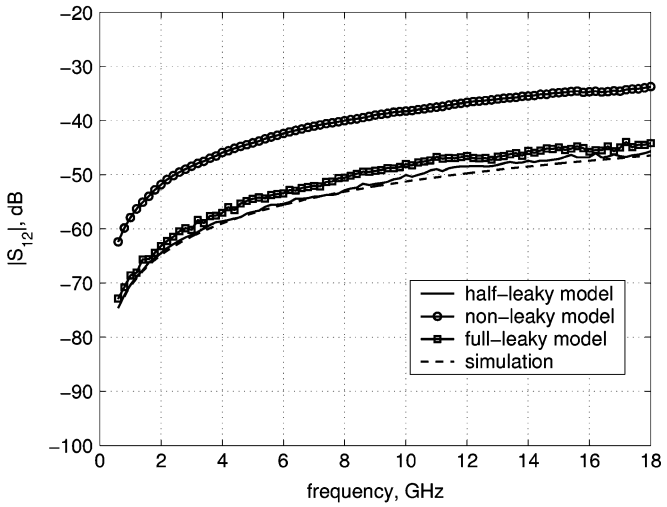

Fig. 12. Near-end crosstalk of the two loose coupled coplanar lines of Fig. 1(a) compared with simulations. These lines are 0.58-mm long, as are the thrus used during calibration.

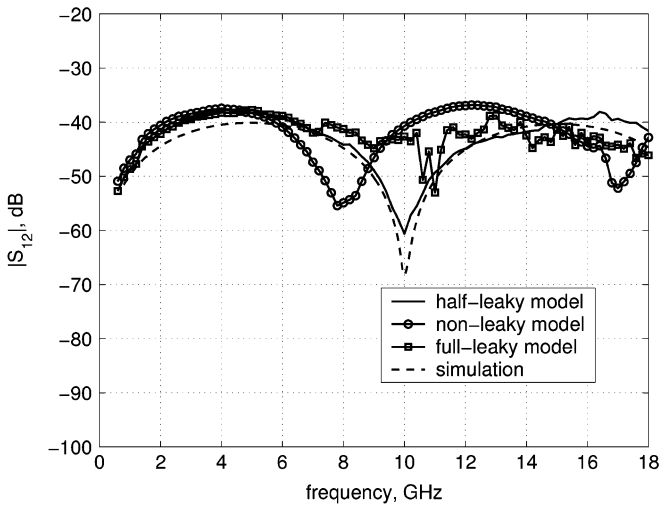

Fig. 13. Near-end crosstalk of the two loose coupled coplanar lines of Fig. 1(a), compared with simulations. These lines are 6.6-mm long, i.e., more than ten times the thrus used during calibration.

crosstalk term by the full-leaky calibration, while the new partially leaky algorithm provides more reasonable measurements.

Figs. 12–14 report measurements and simulations of loosely coupled coplanar lines, connected between ports 1–3 and 2–4, similar to the ones depicted in Fig. 1(a). All the simulations were performed with a commercial simulator, implementing a simple circuital model. Fig. 12 refers to 0.58-mm coupled lines. This is exactly the length of the thrus employed during the calibration. Scattering parameter S_{12}, i.e., the near-end coupling between the two structures, is clearly overestimated by the nonleaky model since it does not include the correction for leakage between ports 1 and 2, while the proposed half-leaky and full-leaky calibrations demonstrate a very good agreement with simulations. Let us now consider the 6.6-mm coupled lines of Fig. 13. The 10-GHz resonance predicted by simulations is found only with the half-leaky model. The effect of the miscorrection of the full-leaky model is evident since this device is much longer than the thrus used during calibration.

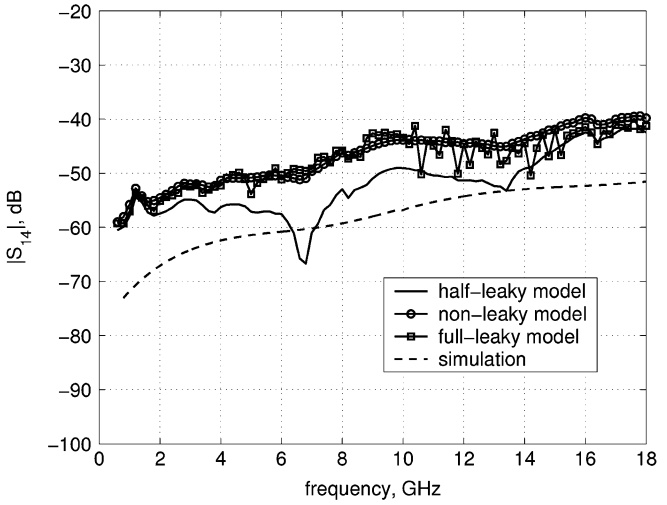

Fig. 14. Far-end crosstalk of the two loose coupled coplanar lines of Fig. 1(a), compared with simulations. These lines are 6.6-mm long.

The nonleaky model is also not able to provide the right value of the resonance frequency. Finally, in Fig. 14, the far-end crosstalk of the same 6.6-mm coupled lines is shown. Also in this case, we notice a better agreement of the half-leaky model to simulation with respect to the other two models.

V. Conclusion

A simple calibration procedure for a half-leaky multiport problem has been presented. The algorithm has exploited an optimized set of calibration standards, which can be easily applied to on-wafer measurements, similar to classical thru-reflect line (TRL) or LRM calibration. Simulations, coaxial, and on-wafer measurements were performed. If applied to multifinger probes, especially when measuring different length devices, the new model shows better performances than classical full-leaky and nonleaky models.

Appendix

Here, an example of implementation of system (3) is given. Let us consider the case of a full-leaky model four-port system. We connect an ideal thru between ports 1 and 3 and two shorts at ports 2 and 4.

The standard model S-matrix has all zero elements, except $S_{13} = S_{31} = 1$ and $S_{22} = S_{44} = -1$ (for simplicity, we consider ideal shorts in this example)

$$\mathbf{S} = \begin{pmatrix} 0 & 0 & 1 & 0 \\ 0 & -1 & 0 & 0 \\ 1 & 0 & 0 & 0 \\ 0 & 0 & 0 & -1 \end{pmatrix}.$$

We write the first two lines (corresponding to indices $i = j = 1$ and $i = 2\ j = 1$) of system (3) in scalar form

$$\begin{aligned} &-M_{11} - S_{m11}L_{31} - S_{m21}L_{32} - S_{m31}L_{33} + H_{31} \\ &\quad + S_{m11}K_{11} + S_{m21}K_{12} + S_{m31}K_{13} = 0 \\ &-M_{21} + S_{m11}L_{21} + S_{m21}L_{22} + S_{m31}L_{23} - H_{21} \\ &\quad + S_{m11}K_{21} + S_{m21}K_{22} + S_{m31}K_{23} = 0. \end{aligned}$$

$$\overbrace{\begin{pmatrix} -1 & \cdots & -S_{m11} & -S_{m21} & -S_{m31} & \cdots & 1 & \cdots & S_{m21} & S_{m31} & \cdots \\ & & & & & \cdots & & & & & \\ & & & & & \cdots & & & & & \\ & & & & & \cdots & & & & & \\ & & & & & \cdots & & & & & \\ & & & & & \cdots & & & & & \\ & & & & & \cdots & & & & & \\ & & & & & \cdots & & & & & \\ & & & & & \cdots & & & & & \\ & & & & & \cdots & & & & & \\ & & & & & \cdots & & & & & \\ & & & & & \cdots & & & & & \end{pmatrix}}^{\mathbf{N}} \overbrace{\begin{pmatrix} M_{11} \\ \vdots \\ L_{31} \\ L_{32} \\ L_{33} \\ \vdots \\ H_{31} \\ \vdots \\ K_{12} \\ K_{13} \\ \vdots \end{pmatrix}}^{\mathbf{u}} = \overbrace{\begin{pmatrix} -K_{11}S_{m11} \\ 0 \\ \vdots \\ \vdots \\ \vdots \\ \vdots \\ \vdots \\ \vdots \\ \vdots \\ \vdots \end{pmatrix}}^{\mathbf{g}} \tag{6}$$

In the same way, one can write all the remaining equations for this and the other standard connections. Each standard connection provides 16 equations and the overall equation set forms the linear system $\mathbf{Nu} = \mathbf{g}$, as in (6), shown at the top of this page, where one of the unknowns, e.g., K_{11}, can be assumed equal to 1.

The same procedure applies to the case of a half-leaky model four-port system, but this time, half of the unknowns are equal to 0, i.e.,

$$\begin{aligned} M_{23} &= M_{32} = M_{24} = M_{42} = M_{13} = M_{31} = M_{14} = M_{41} = 0 \\ L_{23} &= L_{32} = L_{24} = L_{42} = L_{13} = L_{31} = L_{14} = L_{41} = 0 \\ H_{23} &= H_{32} = H_{24} = H_{42} = H_{13} = H_{31} = H_{14} = H_{41} = 0 \\ K_{23} &= K_{32} = K_{24} = K_{42} = K_{13} = K_{31} = K_{14} = K_{41} = 0. \end{aligned}$$

These unknowns no longer will appear in vector $\mathbf{u}$. As an example, the first two equations of the system, for a thru 1–3 and two shorts at ports 2 and 4 now become

$$\begin{aligned} -M_{11} - S_{m31}L_{33} + S_{m11}K_{11} + S_{m21}K_{12} &= 0 \\ -M_{21} + S_{m11}L_{21} + S_{m21}L_{22} - H_{21} + S_{m11}K_{21} + S_{m21}K_{22} &= 0. \end{aligned}$$

and the system

$$\overbrace{\begin{pmatrix} -1 & \cdots & -S_{m31} & \cdots & S_{m21} \\ & & \cdots & & \\ & & \cdots & & \\ & & \cdots & & \\ & & \cdots & & \\ & & \cdots & & \\ & & \cdots & & \\ & & \cdots & & \end{pmatrix}}^{\mathbf{N}} \overbrace{\begin{pmatrix} M_{11} \\ \vdots \\ L_{33} \\ \vdots \\ K_{12} \\ \vdots \end{pmatrix}}^{\mathbf{u}} = \overbrace{\begin{pmatrix} -K_{11}S_{m11} \\ 0 \\ \vdots \\ \vdots \\ \vdots \\ \vdots \end{pmatrix}}^{\mathbf{g}}.$$

ACKNOWLEDGMENT

The authors thank G. Boll, GGB Industries, Naples, FL, for providing the multifinger probes and for the realization of the custom calibration substrate. The authors are indebted to Prof. U. Pisani, Politecnico di Torino, Turin, Italy, for the valuable discussions.

REFERENCES

[1] L. Betts and J. Dunsmore, "High performance characterization of wireless handset front-end modules," in *Proc. Asia–Pacific Microwave Conf.*, vol. 3, Dec. 2001, pp. 1088–1091.

[2] U. Lott, W. Baumberger, and U. Gisiger, "Three-port RF characterization of foundry dual gate FETs using two-port test structures with on-chip loading resistors," in *Proc. IEEE Int. Microelectronics Test Structures Conf.*, Mar. 1995, pp. 167–180.

[3] J.-C. Tippet and R.-A. Speciale, "A rigorous technique for measuring the scattering matrix of a multiport device with a 2-port network analyzer," *IEEE Trans. Microw. Theory Tech.*, vol. MTT-30, no. 5, pp. 661–666, May 1982.

[4] M. Davidovits, "Reconstruction of the s-matrix for a 3-port using measurements at only two ports," *IEEE Trans. Microw. Theory Tech.*, vol. MTT-5, no. 10, pp. 349–350, Oct. 1995.

[5] S. Sercu and L. Martens, "Characterizing n-port packages and interconnections with a 2-port network analyzer," in *IEEE 6th Topical Electrical Performance Electronic Packaging Meeting*, Oct. 1997, pp. 163–166.

[6] H.-C. Lu and T.-H. Chu, "Multiport scattering matrix measurement using a reduced-port network analyzer," *IEEE Trans. Microw. Theory Tech.*, vol. 51, no. 5, pp. 1525–1533, May 2003.

[7] J.-C. Rautio, "Techniques for correcting scattering parameter data of an imperfectly terminated multiport when measured with a two-port network analyzer," *IEEE Trans. Microw. Theory Tech.*, vol. MTT-31, no. 5, pp. 407–412, May 1983.

[8] C. S. Hartmann and R. T. Hartmann, "Software for multi-port RF network analysis with a large number of frequency samples and application to 5-port SAW device measurement," in *Proc. Ultrasonics Symp.*, vol. 1, Dec. 1990, pp. 117–122.

[9] H. Heuermann and B. Schiek, "Error corrected impedance measurements with a network analyzer," *IEEE Trans. Instrum. Meas.*, vol. 44, pp. 295–299, Apr. 1995.

[10] J. Martens, D. Judge, and J. Bigelow, "Uncertainties associated with many-port (>4) s-parameter measurements using a four-port vector network analyzer," *IEEE Trans. Microw. Theory Tech.*, vol. 52, no. 5, pp. 1361–1368, May 2004.

[11] D. F. Williams and D. K. Walker, "In-line multiport calibrations," in *51st ARFTG Dig.*, Jun. 1998, pp. 88–90.

[12] W. Lin and C. Ruan, "Measurement and calibration of a universal six-port network analyzer," *IEEE Trans. Microw. Theory Tech.*, vol. 37, pp. 734–742, Apr. 1998.

[13] J. Helton and R. Speciale, "A complete and unambiguous solution to the super-TSD multiport-calibration problem," in *IEEE MTT-S Int. Microwave Symp. Dig.*, vol. 83, May 1983, pp. 251–252.
[14] M. Schoon, "A semi-automatic 3-port network analyzer," *IEEE Trans. Microw. Theory Tech.*, vol. 41, no. 6, pp. 974–978, Jun. 1993.
[15] W. V. Moer and Y. Rolain, "Proving the usefulness of a three-port nonlinear vectorial network analyzer through mixer measurements," *IEEE Trans. Instrum. Meas.*, vol. 52, no. 12, pp. 1834–1837, Dec. 2003.
[16] F. Sanpietro, A. Ferrero, U. Pisani, and L. Brunetti, "Accuracy of a multiport network analyzer," *IEEE Trans. Instrum. Meas.*, vol. 44, no. 2, pp. 304–307, Apr. 1995.
[17] A. Ferrero, U. Pisani, and K. Kerwin, "A new implementation of a multiport automatic network analyzer," *IEEE Trans. Microw. Theory Tech.*, vol. 40, no. 11, pp. 2078–2085, Nov. 1992.
[18] A. Ferrero, F. Sanpietro, and U. Pisani, "Multiport vector network analyzer calibration: A general formulation," *IEEE Trans. Microw. Theory Tech.*, vol. 42, no. 12, pp. 2455–2461, Dec. 1994.
[19] A. Ferrero and F. Sanpietro, "A simplified algorithm for leaky network analyzer calibration," *IEEE Microw. Guided Wave Lett.*, vol. 5, no. 4, pp. 119–121, Apr. 1995.
[20] J. V. Butler, D. K. Rytting, M. F. Iskander, R. D. Pollard, and M. V. Bossche, "16-term error model and calibration procedure for on-wafer network analysis measurements," *IEEE Trans. Microw. Theory Tech.*, vol. 39, no. 12, pp. 2211–2217, Dec. 1991.
[21] H. V. Hamme and M. V. Bossche, "Flexible vector network analyzer calibration with accuracy bounds using an 8-term or a 16-term error correction model," *IEEE Trans. Microw. Theory Tech.*, vol. 42, no. 6, pp. 976–987, Jun. 1994.
[22] K. Silvonen, "LMR 16-a self-calibration procedure for a leaky network analyzer," *IEEE Trans. Microw. Theory Tech.*, vol. 45, no. 7, pp. 1041–1049, Jul. 1997.
[23] H. Heuermann and B. Schiek, "Calibration of network analyzer measurements with leakage errors," *Electron. Lett.*, vol. 30, no. 1, pp. 52–53, Jan. 1994.
[24] R. Speciale, "A generalization of the TSD network-analyzer calibration procedure, covering n-port scattering-parameter measurements, affected by leakage errors," *IEEE Trans. Microw. Theory Tech.*, vol. MTT-25, no. 12, pp. 1100–1115, Dec. 1977.
[25] V. Teppati, A. Ferrero, D. Parena, and U. Pisani, "A simple calibration algorithm for partially leaky model multiport vector network analyzers," in *65th ARFTG Dig.*, Jun. 2005, pp. 1–4.

Valeria Teppati (S'00–M'04) was born in Turin, Italy, on October 2 , 1974. She received the Electronics Engineering degree and Ph.D. in electronic instrumentation from the Politecnico di Torino, Turin, Italy, in 1999 and 2003, respectively.

Since 2003, she has been a Research and Teaching Assistant with the Politecnico di Torino. Her research interests and activities include microwave devices design, linear and nonlinear measurements design, calibration, and uncertainty.

Andrea Ferrero (S'86–M'88) was born in Novara, Italy, on November 7, 1962. He received the Electronic Engineering degree and Ph.D. degree in electronics from the Politecnico di Torino, Turin, Italy, in 1987 and 1992, respectively.

In 1988, he joined Aeritalia as a Microwave Consultant. During 1991, he was a summer student with the Microwave Technology Division, Hewlett-Packard, Santa Rosa, CA. In 1995, he was a Guest Researcher with the Electrical Engineering Department, Ecole Polytechnique de Montrèal, Montrèal, QC, Canada. In 1998, he became an Associate Professor of electronic measurements with the Politecnico di Torino. His main research activities are in the area of microwave measurement techniques, calibration, and modeling.